

Electromagnetic and Thermal Modeling of a Permanent Magnet Synchronous Machine with Either a Laminated or SMC Stator

David K. Farnia
Burgess Norton Mfg.
Geneva, IL 60134
dkfarnia@burgessnorton.com

Tetsuya Hattori
JRI Solutions, Limited
Tokyo, Japan

Abstract--- This paper will cover the electromagnetic and thermal simulation of a large PMSM. First the electromagnetic simulation will verify the simulated electromagnetic properties match the measured electromagnetic properties. Metrics such as torque and back EMF will determine the accuracy of the simulation. Next JMAG's iron loss tool and thermal modeling package will then simulate losses and thermal behavior. These results are compared to the measured losses and thermal properties of the motor.

The loss modeling forms a visual representation of the temperature distribution within the motor. This will go beyond what the thermocouples can measure and actually show how the heat is forming and dissipating. The information will aid in the determination of hot spots within the motor, which will lead to design modifications for the next motor design.

This paper will discuss simplifications to the modeling and how they affect the results. Even with simplifications the final results will be indicative of how the motor performs. It will also provide a method to test hypotheses on the design without building a working prototype. This will allow numerous design iterations in a relatively short time for considerably less cost. The end result is the next generation of this motor will utilize results from both physical testing and simulation to create a design that draws on theoretical and physical results.

Unfortunately due to time constraints the SMC motor comparison can not be included in this paper since the testing has not been completed.

I: INTRODUCTION

The following paper presents a study of a permanent magnet synchronous machine (PMSM). Two versions of the same design are to be constructed, one with a stator comprised of traditional electrical steel laminations, and a second with a stator constructed of soft magnetic composites (SMC). The laminated motor is a more conservative approach for the application, while the SMC motor is more experimental, it will utilize several features that will make it less expensive and more efficient. The motors are designed for a large traction application and each design will be evaluated based on the same criteria. The motor

manufacturer has asked not to have the purpose of the motor, nor specifics about the controller disclosed.

The application initially utilized an induction machine, but it had a poor efficiency over its operating speed range. In order to improve the efficiency, the induction machine is replaced by a PMSM designed to provide a wide operating range and necessary torque for the application while achieving a higher efficiency. The motor was initially designed using a laminated stator; however, early in the design process it was clear that an SMC stator would be feasible as well as beneficial at the higher operating speeds. The SMC design could utilize copper reducing geometries, as well as offer lower losses at medium and high frequencies.

The use of a PMSM in this application has been made possible by two factors, the reduction in permanent magnet cost, and improvements in controller technology. Taking this into consideration, the motors will use surface mounted Neodymium Iron Boron permanent magnets as well as a unique controller algorithm. The algorithm is designed to maintain the operating temperature below 165° C to ensure that the coils do not overheat. The controller will command different currents based on the motor loading. This results in a non traditional torque speed curve.

The SMC stator design is an option due to the motor's operation at higher frequencies, where the SMC stator will have lower iron losses than the laminated stator. The use of SMC in electrical applications has been gaining in popularity in recent years as improvements in the material's magnetic and mechanical properties combined with its 3D shape capabilities offer new design options. In this application SMC has several advantages. First, since it is pressed into individual components and then stacked, there is very little stack up error. This allows tighter tolerances, and reduces variation from motor to motor. Second, the formation of complex geometries is possible due to the three dimensional shape characteristics and isotropic flux capabilities. This translates into extended back iron and tooth tips so the end windings can be buried in the stator. A stator tooth end with the extended back iron and tooth tip is shown in Figure 1.



Figure 1: Single tooth with extended back iron and tip.

It is also possible to create a single tooth and assemble these teeth to form the stator. A single tooth would be comprised of two end sections as shown in Figure 1. Finally, since each tooth can be formed separately and thus would separately, there will be a higher fill factor for the copper windings. These factors coupled with the performance at medium to high frequencies make the SMC design an attractive alternative. Figure 2 shows how the single tooth sections are assembled to form the stator.

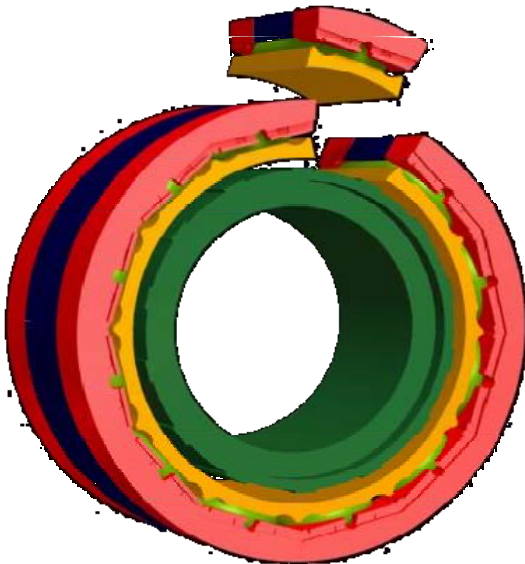


Figure 2: Single tooth wound as it would fit into the stator.

Both motors will be tested and evaluated in a similar fashion at the motor designer's test facilities. Some details of the testing and motor design will not be covered at the request of the motor manufacturer. Also, simplifications to

the design to reduce the complexity of the model thus reduce the analysis time are made in order to focus the research on the electromagnetic and thermal design. The most obvious of these is the controller and power electronic simplification. The motor simulation will use values taken from measurements of the actual motor under test. These values will be used by the simulation to calculate performance parameters for the thermal simulation such as flux density, current density, and losses. The thermal simulation will use coefficients of thermal conductivity that will take the coolant oil into consideration and set appropriate values to the surfaces that are in contact with the coolant oil. These coefficients will take convective flow into consideration, although, convective flow can not be simulated its affects can be approximated.

II. ORIGINAL DESIGN SPECIFICATIONS

The motor will be used in a large traction application. This application requires heavy duty loading both thermally and electromechanically. To do this the motor will be enclosed by a case with coolant running through the stator. A rendering of the motor with end rings and a case around the stator is shown in Figure 3.



Figure 3: CAD rendering of motor.

The motor will use a concentrated pole stator winding which will allow individually wound teeth, and in the case of the SMC design the teeth can be wound separately leading to a better fill factor. A picture of the wound laminated stator is shown in Figure 4.



Figure 4: Wound laminated stator.

There will be some slight differences between the laminated design and the SMC design these are shown with several other physical parameters in Table 1.

Table 1: Physical parameters of the motors.

Parameter	Laminated Design	SMC Design
Stack height	152 mm	160 mm
Total height	204 mm	160 mm
Stator slots	12	12
Rotor poles	14	14
Stator OD	365.5mm	365.5mm

The biggest difference between the SMC design and the laminated design is the height. Since the SMC motor utilizes buried winding, the stack height and total height are the same. Since the windings are buried in the motor the effective length of the SMC motor is 160mm and isn't reduced by the buried windings.

Both of the motors will have a three phase wye connection, with the same number of turns per coil. However, there will be a difference in coil resistance do to winding length. The operating speed of the motor is anywhere from 0-4000 rpm, or electrical frequencies from 0 to 466.7Hz.

III. ANALYSIS STEPS

Initially the motor was designed with linear simulations in order to define the physical parameters such as the tooth width, number of poles, number of turns, etc. Since motor simulation is an iterative process, it was necessary to first create a two dimensional model of the motor to allow short simulation times. This model will ensure all the parts of the

simulation are in place and result in an accurate model. The size of the 2D simulation allows quick run times and rapid changes that can weed out any errors in the motor model.

The next step uses the conditions from the 2D model and translates that into a 3D model. Using JMAG's CAD import feature the CAD model is brought into the JMAG environment. Even with improvements in processor speed and modeling equations, 3D models are still time consuming, so getting the model's conditions correct is a valuable time saving tool.

To set the conditions for the loaded model, an open circuit simulation will obtain the back EMF waveforms as well as cogging torque. Since the Back EMF is a function of initial rotor position, the open circuit simulation will be run in both 2D and 3D since each model will have a different initial rotor position. The loaded cases are simulated using the phase angle of the back EMF to set the current phase angle and amplitude. Since the controller is not simulated, the amplitude and phase angle of the current must be manually set in JMAG. It is assumed that the back EMF voltage is lagging the phase voltage by certain number of degrees that is a function of the controller algorithm. From the measured data the voltage and current amplitude are known, and the power factor angle can be calculated. The phase angle of the current is determined relative to the back EMF phase angle which was determined in the open circuit model.

Each simulated test point will consist of a speed, current amplitude, and current phase angle relative to the back EMF phase angle. For the electromagnetic simulation the coil resistance is held constant, but for the thermal simulation the coil resistance will change due to its dependence on temperature. Initially, however, a constant coil resistance will give a fairly good approximation for electromagnetic performance.

There are three types of loss within the system, iron loss of the stator and rotor, joule loss of the coil, and eddy current loss within the magnets. The electromagnetic simulation determines the flux density distribution of the motor; this is used by the Iron Loss tool to determine iron loss in the steel. Adding the coil's joule loss and magnet loss from the electromagnetic simulation to the iron loss from the Iron Loss tool, the total loss is calculated and compared to measured losses. If these two values are in agreement the simulated losses are then used to calculate the thermal response of the machine.

The machine's thermal response will use the losses at heat sources and create a finite element model of the motor's temperature rise. Since the thermal time constant is much longer than the electromagnetic time constant, the losses over one electrical cycle are averaged and used as the base

loss of the thermal simulation. Initially a static thermal simulation with the rotor removed is used to compare with the measured results. The static results can show hot spots and give an estimation of temperature response in the machine as well as acting as an indicator of the thermal circuit's accuracy. The transient thermal model is then run if the static analysis is in agreement with measured temperatures.

IV. TWO DIMENSIONAL FEA

The 2D model is created within the JMAG modeling environment, the 2D JMAG model is shown in Figure 5.

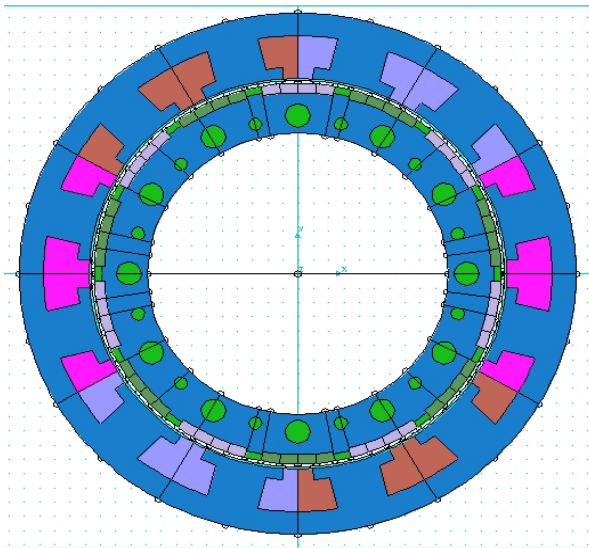


Figure 5: JMAG 2D model of a 3 phase 14 pole, 12 slot, PMSM.

Since the 2D model is used to analyze the SMC as well as the laminated design, the divisions to create a single tooth are added. The SMC design will require a 3D analysis to fully capture the performance, but the 2D analysis provides the starting point. The conditions of the model are set as well as the material properties. The model will use a non linear BH curve for the steel and a linear approximation for the magnets.

Since the controller is not simulated, the electrical circuit is fairly simple, as shown in Figure 6.

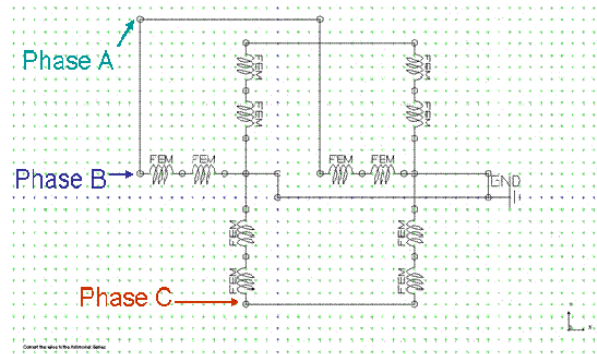


Figure 6: JMAG motor circuit, 3 phase, 12 coils.

The above figure shows the open circuit condition. The loaded condition will use a 3 phase current source as an input to the three labeled points. With the circuit and the model in place, the simulation proceeds to determine the open circuit results.

A. 2D Open Circuit Results

Since the simulation ran parallel with motor development, test data collection and analysis against model data was an ongoing process. Back EMF data was initially collected and compared to the simulated results. Verification that each phase had equal measured EMF magnitude meant that there were no problems with the windings and that comparing one phase is sufficient for analysis. JMAG's simulated back EMF versus rotor angle at 500 rpm is shown in Figure 7.

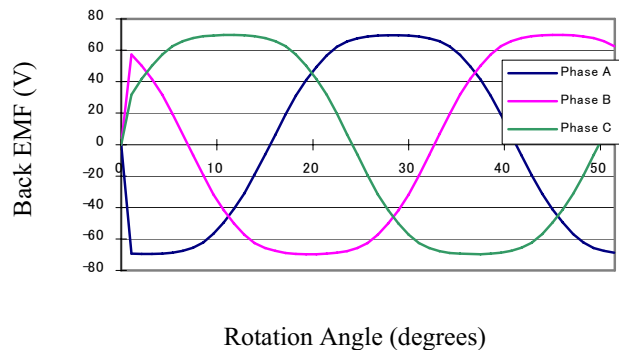


Figure 7: Simulated back EMF voltage versus position, 500 rpm, 2D

A comparison of simulated peak back EMF measurements against measured results at different speeds shows little difference in amplitude. The results for the simulated back EMF amplitude compared to the measured are shown in Figure 8.

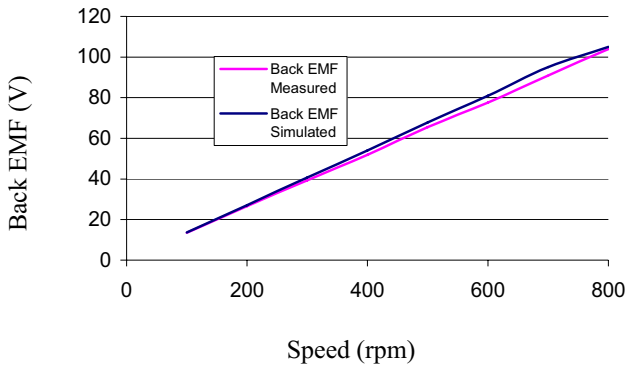


Figure 8: Measured back EMF voltage, 2D simulated back EMF voltage versus speed.

From the above figure it is apparent that the simulated back EMF is very close to the measured back EMF, the difference is within a maximum of 5%. This would lead to the assumption that the open circuit motor simulation performance is in line with the actual motor performance, and therefore the model's physical parameters and base circuit are correct. The next step is to run the model under load.

B. 2D Excited Motor Results

Since the focus of the study is on electromagnetic and thermal simulation the controller is not simulated. Instead the motor will be excited by ideal sources which will approximate the actual controller. The basis for the excitation is discussed above. Below 2000rpm the motor will use a PWM sine wave current for torque control, above this speed the controller goes to a six-step current waveform. The PWM is approximated by an ideal sinusoidal current, and the six step controller uses a square wave current.

After the current amplitude, phase angle, and speed are set JMAG calculates the torque, flux density, air gap flux, etc. The torque waveform will be averaged to determine the approximate steady state torque. The simulated average torque compared with measured torque versus speed is shown in Figure 9.

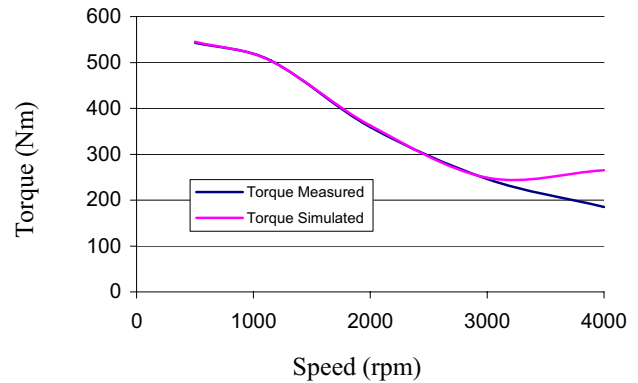


Figure 9: Measured torque, simulated torque, versus speed 2D model.

Some difficulties with the controller approximation are encountered at this point. Since the controller will go into six step above 2000 rpm the voltage waveform will become more distorted as rotor speed increases. Typically at higher speeds the voltage waveform would need to be broken down with a Fourier analysis to determine the fundamental and use that value to calculate the current phase angle. This was not done during this round of testing. The distortion of the voltage waveform at high speeds is most likely responsible for the torque difference at the higher speed points. However, at the lower speeds the simulated torque comes very close to the measured torque, therefore the controller simplifications still captures the medium and low speed motor dynamics and the parameters of the simulation are representative of the motor.

The next metric that is examined is the flux density of the motor. This ensures that the motor is operating within its expected magnetic load range. The flux density of the 2D model is shown in Figure 10.

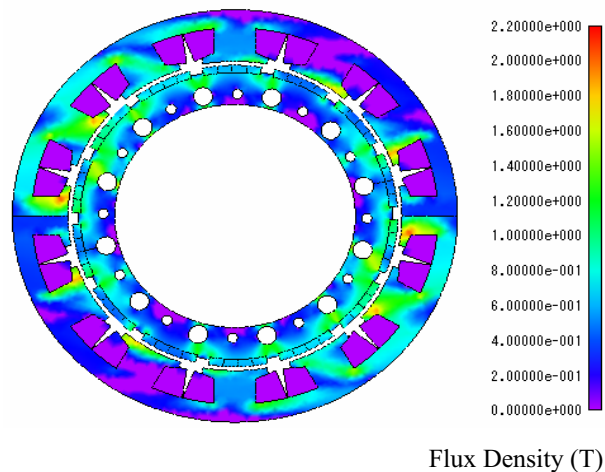


Figure 10: Flux density in JMAG, 500 rpm, 266A current, 2D.

Since the flux densities are within their expected values, it would appear that the circuit is working properly and that the simulation is capable of modeling the machine. Since the 2D model doesn't capture all the dynamics of the machine, the 3D model will add the remaining detail and insight to the analysis.

V. THREE DIMENSIONAL FEA

A. Initial Set-up

Analyzing the model in 2D gives a very good approximation for the laminated design, but the thermal model and the SMC model will require a 3D FEA. The 3D model in JMAG is shown in Figure 11.

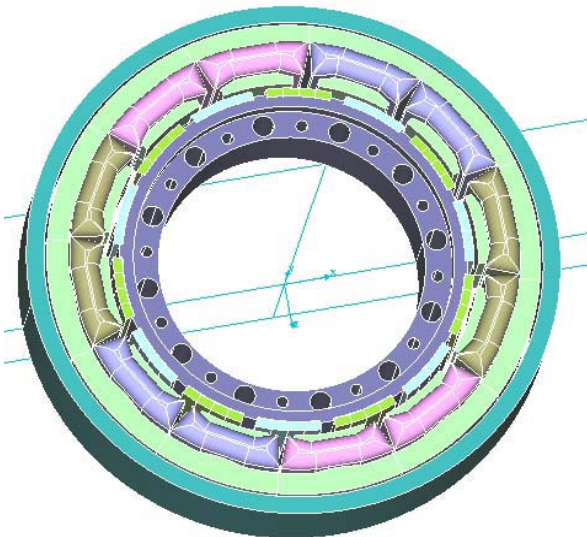


Figure 11: Motor model in JMAG 3 phase, 12 slot, 14 pole.

In the 3D model the windings are created in the CAD program and approximated to fill the entire winding space. This approximation has some flaws, however. Even though the coils fill up the entire slot, there are air gaps between the strands of copper. This will have little effect on the electromagnetic simulation, but will have ramifications for the thermal model. Since modeling each turn of a coil is not a reasonable solution an approximation is necessary in the thermal circuit.

The remaining conditions are set based on the results of the 2D analysis and using the same material data as was used in that analysis. As with the 2D model, the first simulation is an open circuit model to determine back EMF phase angles.

B. 3D Open Circuit Results

The first run of the 3D model is to determine the back EMF waveforms and their phase angles. Since the rotor will be aligned in a different position compared to the 2D model the back EMF phase angle will be different; the waveform is shown in Figure 12.

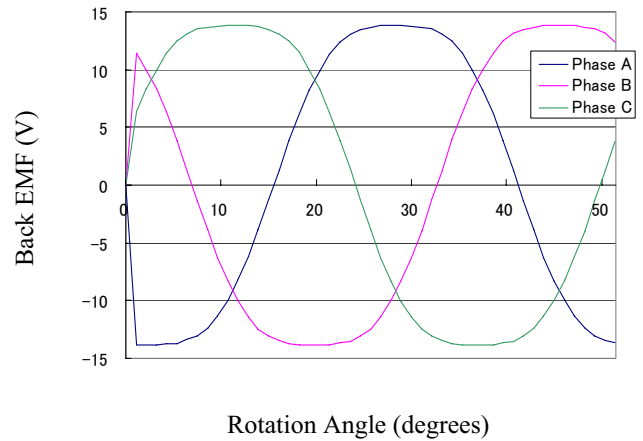


Figure 12: Back EMF voltage versus position, 100 rpm, 3D model.

Again the simulated and measured back EMF amplitude versus speed is compared to determine model accuracy; this is shown in Figure 13.

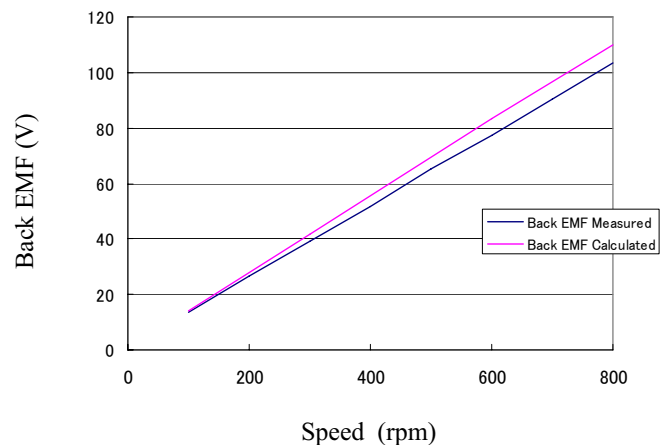


Figure 13: Measured back EMF voltage, simulated back EMF voltage versus speed, 3D model.

The model appears to have an increasing drift from the measured data; however, this is only 7.5% at its maximum.

It appears that the model has similar open circuit results as the 2D model, which would lead to the assumption that the conditions have been set correctly. The next step becomes determining the loaded results for the motor.

C. 3D Excited Motor Results

The 3D model will use the same loading as the 2D model. So the 3D model will use the same current amplitude as the 2D model, however, the phase angle for the 3D model will come from the 3D back EMF calculation. The results of the torque versus speed for the 3D model versus the measured data are shown in Figure 14.

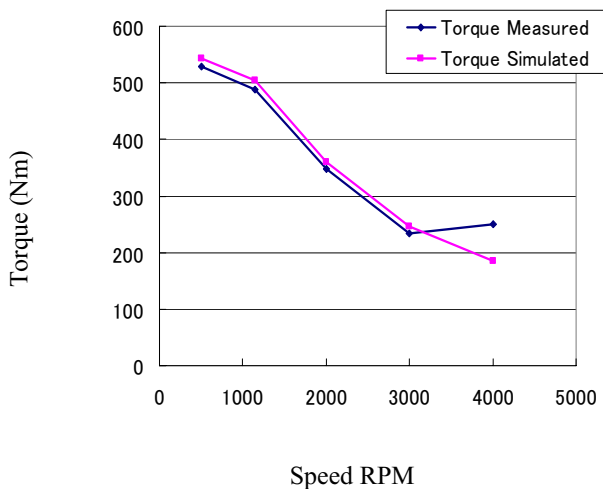


Figure 14: Measured torque, simulated torque, versus speed 3D model.

As with the 2D model there is some error at the higher speeds due to the distortion of the voltage waveform. This results in the higher value of the simulated torque. However, since the simulated torque is very close to the measured torque at low and medium speeds the 3D losses and thermal model are calculated. If the simulation is correct, the model can be used to estimate the losses. To do this the joule loss of the coil and magnet eddy current loss are added with the iron loss. The joule loss and magnet eddy current loss are calculated in the electromagnetic simulation, but the iron losses must be calculated with the Iron Loss tool in JMAG. The Iron Loss tool will use the flux density distribution from the electromagnetic simulation to determine an iron loss distribution. The 3D flux density is shown in Figure 15.

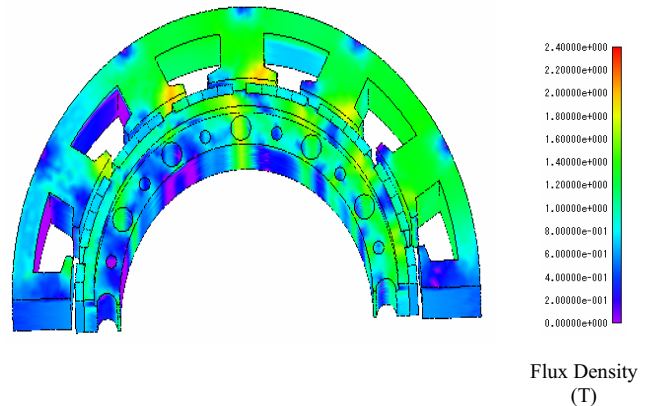


Figure 15: 3d flux density in JMAG, 500 rpm, 266A current, 3D model.

From the flux density model JMAG's Iron Loss tool will calculate the iron losses in the rotor and the stator. Figure 16 shows a physical representation of the iron losses of the model.

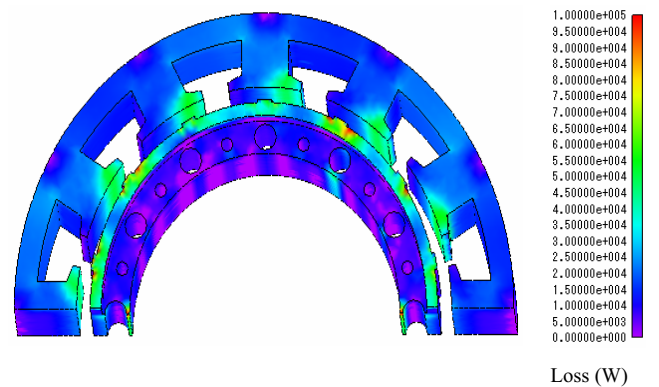


Figure 16: 3d iron loss (hysteresis+eddy current) in watts, 3D model.

The last portion of the losses occur in the magnets. The magnets are split into sections to reduce the eddy currents, but they still contribute to the total loss. Figure 17 shows a model of the eddy current loss in the magnets.

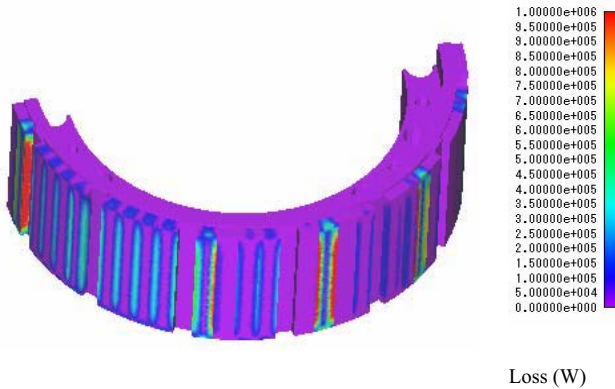


Figure 17: 3d eddy current loss of the magnets in watts.

The total losses of the motor are the sum of the iron losses (including magnet eddy current loss) and the joule loss of the coils. This value can then be compared to the measured losses as a function of frequency. A comparison of the simulated losses versus the measured losses is shown in Figure 18.

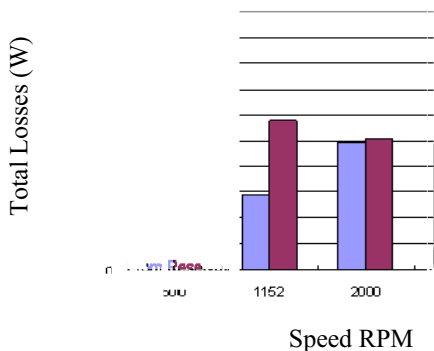


Figure 18: Calculated total loss, measured loss, versus speed, 3D model.

The losses appear to be off from the measured losses. It would appear that in terms of loss modeling the controller approximation is not correct. This error arises from the fact that the current was set to have zero phase shift off the back EMF phase. In other words instead of using the measured current amplitude at a phase angle, the current amplitude was calculated as the portion that was in phase with the back EMF, and therefore the phase shift from the back EMF phase was zero. The simulation calculates the torque correctly because the current that would create torque is set correctly, but it doesn't capture the total current within the machine and therefore doesn't capture all the losses. It also must be noted that JMAG does not simulate the friction and windage losses of the motor, so the results will have some degree of error already built in.

VI. THERMAL ANALYSIS

A. Initial Parameters

The thermal analysis will utilize the model created in 3D to approximate the temperature rise of the motor. The stator will use coolant flowing through the end rings. The coolant will be collected in a reservoir and then circulated through the stator. The reservoir will act like a heat sink to pull the heat off the coolant before recirculation. The flow of the coolant is very important to the motor's thermal regulation capabilities, therefore any insight into hot spots will aid in the motor design. The coolant path for the stator is shown in Figure 19

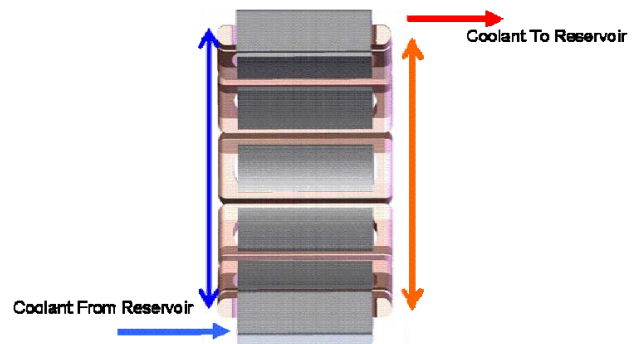


Figure 19: Coolant flow path in the stator.

The coolant will flow from the reservoir into the bottom end of the stator; it will then circulate around the end rings and coils. From here it will flow through the stator slots and to the other side where the end ring will direct the coolant to the exit and toward the reservoir.

In order to monitor the temperature of the motor, thermocouples are installed on the prototype. These will be used to determine the local heating of the stator. This is necessary because the circulation of the coolant causes a non uniform temperature distribution in the coils. The temperature will be dependant on where the coil is located with respect to the entrance and exit of the coolant. To monitor temperature, there are 6 thermocouples in various locations along the stator coils; these are shown in Figure 20.

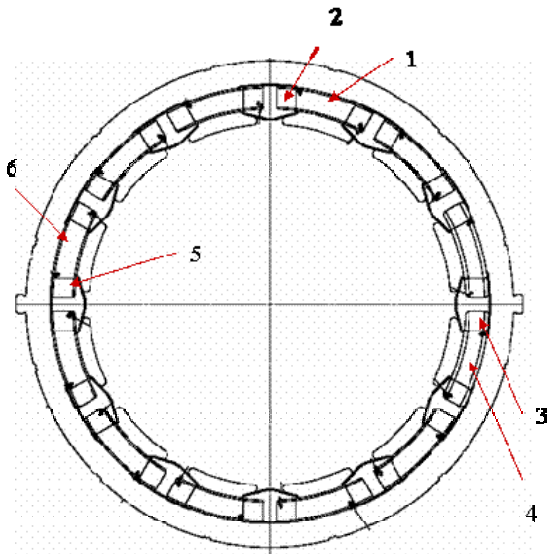


Figure 20: Location of the 6 thermocouples along the stator.

Thermocouple #1 is located at the top of the coil closest to the exit port, with #2 half way up that coil. As expected these will be the two hottest thermocouples since they are at the oil exit, and therefore will encounter the heated oil from all the other coils. Thermocouple #3 and #5 are located half way up the coils at 90 degrees from the exit (and entrance) port. Thermocouples #4 and #6 are located on the top of the coil at the same side that the entrance port is on.

The motor is run until the temperatures of each thermocouple reach steady state. There is a transient portion of the temperature profile, which can be compared with the dynamic simulation, and a steady state portion, which can be compared to the stationary simulation.

B. Modeling and Sensitivity

Due to the difficulty in determining the parameter value in a thermal analysis a sensitivity model is created to show how the thermal parameters will react to temperature rise. This investigation of sensitivity measures several positions on the stator coil that are simulated as if the rotor is removed.

The results of the sensitivity analysis will determine how much accuracy can be attributed to the temperature rise at that position. Three evaluation points and parameter sensitivity to temperature rise are shown in Figure 21.

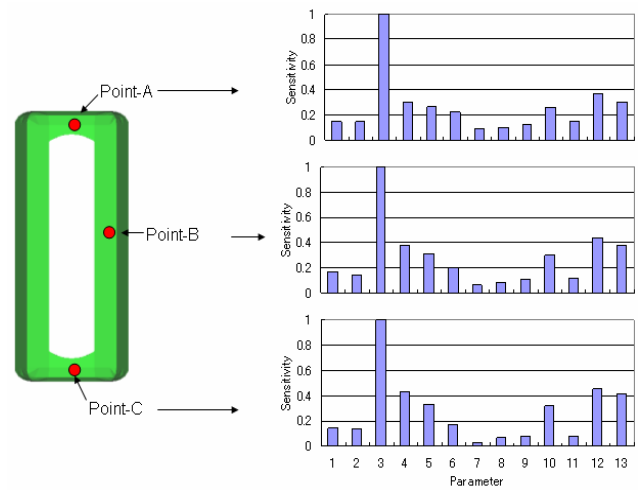


Figure 21: Sensitivity of the thermal parameters, 3D model, rotor removed.

The above parameters come from the 3D model's thermal equivalent circuit. The circuit is an approximation of the heat flow in the motor. The equivalent circuit is shown in Figure 22; the numbered nodes correspond to the sensitivity study in Figure 21.

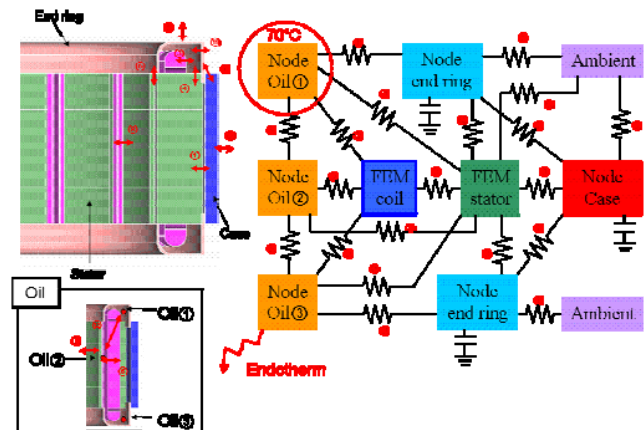


Figure 22: Thermal equivalent circuit of the stator and no rotor, with numbered nodes corresponding to the sensitivity study.

From the sensitivity study the most sensitive parameter is the thermal coefficient between the coil and the coolant inside of the end ring. The next most sensitive coefficients are the in the components connected to the coolant. This would indicate that any component that is directly connected to the coolant is important and caution should be taken when estimating component temperatures that are in direct contact with the coolant.

C. Stationary Analysis

The results of the stationary analysis are used to determine if the thermal circuit is correctly modeling the motor. The thermal profile of the stator without the rotor is shown in Figure 23.

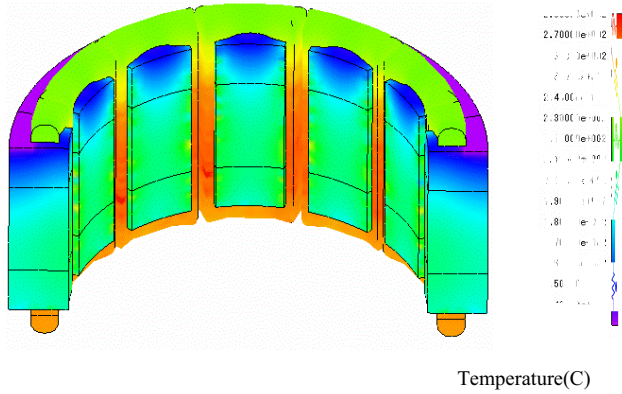


Figure 23: Temperature distribution, stationary analysis, removed rotor, 368A, 100Hz.

The next model in the stationary analysis will include the effects of the rotor. The rotor will remain stationary, but the current frequency will be set as if the rotor were in motion. In order to ensure an accurate representation without unnecessary component modeling the case, end ring, rotor flange, fiber glass band sealing off the stator, gap air, and rotor inner air are modeled in the thermal equivalent circuit. This provides the essential components while minimizing the analysis time. The thermal equivalent circuit is shown in Figure 24.

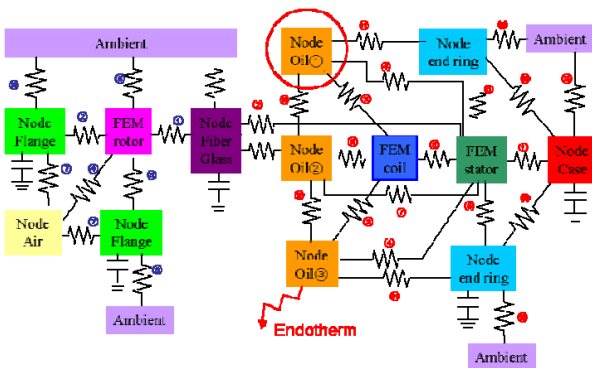


Figure 24: Thermal equivalent circuit.

Temperature rise has an effect on resistance in all components. The temperature dependence of the copper's resistance will have an effect on the coil resistance which will in turn have an effect on current and therefore overall temperature rise. Unfortunately, an analysis that takes the temperature dependence of resistance into consideration

would take too much time. Because of this the resistance of coil is set to its value at 120°C.

The heat capacitor has nothing to do with stationary analysis, but since it is necessary in the transient analysis it is included to maintain congruency between the two thermal circuits.

The temperature of the coolant is modeled with three nodes. These nodes are located at the entrance point, middle point, and exit point (refer to oil node 1-3 in Figure 22). In reality there is a temperature distribution of the coolant, but modeling this distribution would involve the creation of multiple nodes at various positions in the coolant path. For this simulation, an approximation of coolant temperature based on three locations is adequate.

The air gap between the rotor and stator is modeled by thermal equivalent circuit with a convection coefficient that is calculated by the following formula. [1]

$$h_1 = \frac{6.6}{10^5} \frac{vr^{0.67}}{lg^{0.33}} \quad [1]$$

In the above formula vr is the velocity of the air in (cm/sec) and lg is the length of air gap in (cm).

Using the thermal circuit from above the stationary temperature distribution is simulated, this is shown in Figure 25.

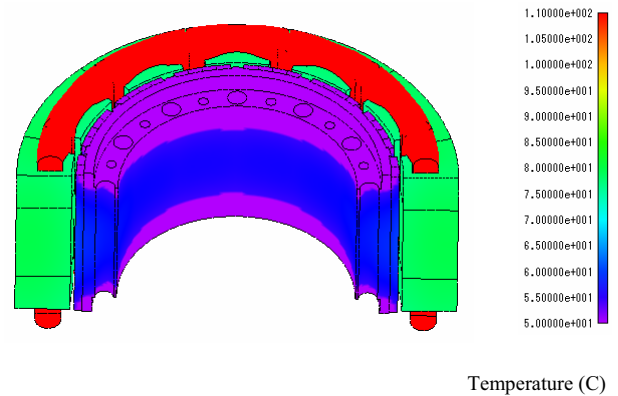


Figure 25: Temperature distribution 500 rpm (58.33Hz), 266A current, 3D model, stationary.

From this analysis the coils can be examined in depth. This will show where the hot spots occur and what their relative heating is. The half section of the coil is shown in Figure 26.

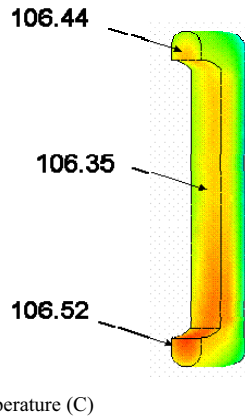


Figure 26: Temperature distribution of a single coil 500 rpm (58.33Hz), 266A current, 3D model, stationary.

The stationary temperature analysis shows that there is a temperature distribution of the coils, but it is much smaller than the gradient that was measured in the motor tests. The coil above corresponds to a coil away from the exit port (exit port has a much hotter temperature and is not representative of the majority of the coils), so the low temperature (corresponded to the coolant entrance side) was measured at 98°C and the high temperature (corresponding to the coolant exit side) was measured at 110°C. The simulated values are approximately an average of this. This is due to the fact that the fluid modeling is approximated by three nodes that are interconnected. In order for JMAG to model the gradient a much more rigorous analysis of the fluid dynamics would be necessary.

The same phenomenon occurs at 3000rpm. The thermal profile of the coil is shown in Figure 27.

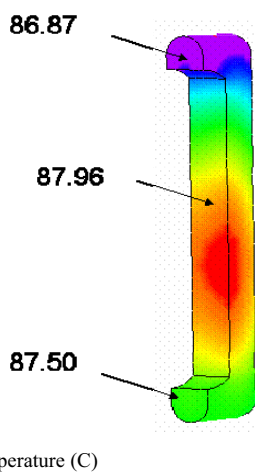


Figure 27: Temperature distribution of a single coil 3000 rpm (350Hz), 90A current, 3D model, stationary.

The measured temperature on the entrance side of the coil is 86°C and 93°C at the exit side. The calculated value is approximately 88°C, which corresponds to an average of the measured gradient.

Even though the temperature gradient can not be modeled, the simulation still provides valuable data on temperature rise and hot spot formation. With more work, a model taking the temperature gradient into consideration can be created and give greater insight into how the motor functions.

D. Transient Analysis

The transient analysis will build on the stationary analysis and show the temperature rise in the motor. However, the transient analysis will not take the temperature dependant magnetic or the temperature dependant resistance into consideration so the calorific value isn't changing. The following analysis will compare the temperature value of the three nodes used to model the coolant (entrance port, middle, and exit port) to the corresponding measured values. The variation of temperature in these nodes is shown in Figure 28 as compared to the measured values.

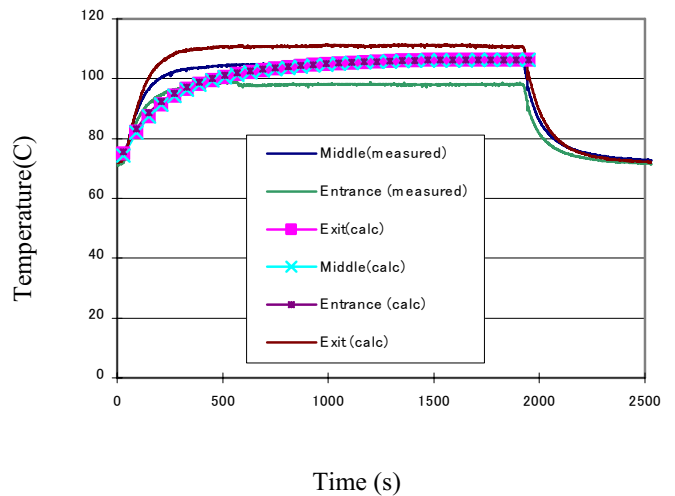


Figure 28: Variation of temperature in the three coolant nodes as compared to the measured values at entrance and exit.

As was the case with the stationary analysis the temperature of the coils is not a gradient, it is an average of the entrance and the exit. Therefore the simulated thermal profile is an average of the measured temperature data. However as seen above the average value would correspond to the middle of the coil. If there were no fluid flow this would correspond to the hottest point in the coil. Knowing this temperature the cooling can be designed to maintain this value below a certain temperature to ensure that the motor will not overheat.

As with the stationary analysis the difficulty lies in modeling the fluid dynamics. The equivalent circuit approximation yields a good average value, but can not model the gradient.

VII. CONCLUSIONS

This paper presents an electromagnetic and thermal simulation of a PMSM. The simulation utilizes finite elements as well as a thermal equivalent circuit to model the motor's response to loading. It has been shown that JMAG is capable of modeling the electromagnetic portions of a motor, and that it can give insight into the thermal modeling as well.

The largest errors occur when approximations are made; unfortunately this will be part of any motor modeling. If the effects of these approximations are known, they can be accounted for. The two sources of error within this model were the controller approximation and the coolant approximation. However, upon completion of the model these two approximations can be improved in the next model.

To improve the controller approximation the current should be set with the phase angle relative to the back EMF. This model reduced the amplitude of the current and aligned it with the back EMF phase angle. Also at higher speeds the measured voltage will have to be broken down by Fourier analysis to determine the fundamental. This amplitude will then be used in the power factor angle calculation.

To improve the thermal model approximation there must be an improvement in how the coolant is modeled. This would most likely either involve creating more coolant nodes, or making the nodes more independent. Creating more nodes would increase the simulation time, so this is not the preferred method. Modify the assumption would involve making the nodes function more independently. For instance create a lower thermal resistance between the coolant node at the entrance and the reservoir coolant node, and a higher resistance between the entrance coolant node and the middle coolant node.

Even with the approximation errors, the model still provides valuable information on the functioning of the motor. The torque and other electromagnetic properties are very close, and the thermal data provides a good idea of the average temperature of the coils.

This information can be utilized in the next motor design to simulate possible motor designs without having to build them. It can also be used for this design to spot problem areas that may be fixable without a redesign. Taken together JMAG has shown that it is a valuable tool for both the electromagnetic as well as thermal modeling of a machine.

VIII. REFERENCES

[1]Thermal Analysis of Soft Magnetic Composite Motors Using a Hybrid Model with Distributed Heat Sources

YouGuang Guo ...

IEEE Transactions on magnetics , vol41,No.6,June 2005